where $2x_0$ is the separation of the two solitons, 2Θ the input collision angle, and ψ_0 is the input soliton shape. One of the most interesting phenomenon is the possibility of beam fusion under certain conditions. As an example, Fig. 3 shows the collision of two solitons of the upper solution branch with the parameters γ = 0.4, ρ_0 = 42, Θ = 0.1, x_0 = 5. As seen after collision, both solitons fuse to a single beam, which, as a kind of higher-order spatial 2-D soliton, periodically changes its shape. Using the invariants of the Eq. (1), the soliton fusion can be interpreted as an analogy of mass defect in nuclear fusion.

1. M. Segev *et al.*, Phys. Rev. Lett. **73**, 3211 (1994); M. D. Iturbe-Castillo *et al.*, Appl. Phys. Lett. **64**, 408 (1994); M. Shin *et al.*, Electr. Lett. **31**, 826 (1995).
2. S. Gatz, J. Herrmann, J. Opt. Soc. Am. B **8**, 2296 (1991); IEEE J. Quant. Electr. **20**, 1732 (1992).

QThH3 **3:15 pm**

Transient self-bending of laser beam in biased photorefractive $Bi_{12}TiO_{20}$ crystal

P. A. Márquez Aguilar, J. J. Sánchez-Mondragón, S. Stepanov, V. Vysloukh, *INAOE, Apartado Postal 51 y 216, Puebla, 72000, Mexico*

Here we report, to our knowledge for the first time, the transient self-bending of the laser beam in photorefractive crystal (PRC) biased by the external DC electric field. The effect is ensured by the dynamic shift of the photocarrier distribution from the beam area under the influence of the driving electric field. As a result, at the beginning of illumination

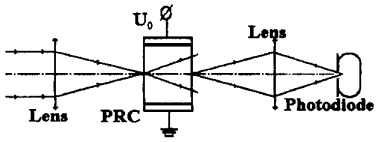

QThH3 Fig. 1 Optical configuration for observation of transient self-bending in photorefractive crystal.

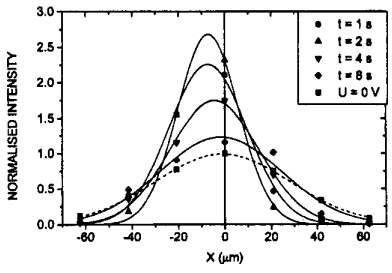

QThH3 Fig. 2 Temporal behavior of the output beam profile along direction of application of external electric field in experiments with BTO samples at λ = 633 nm (approximation by Gaussian curves).

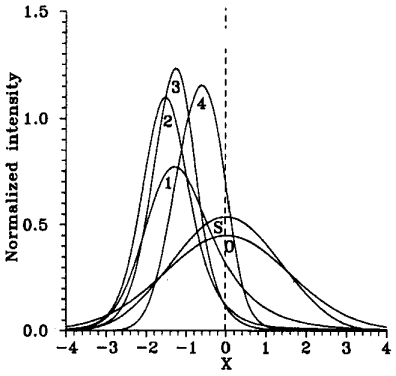

QThH3 Fig. 3 Temporal behavior of the output beam profiles, numerical simulation, 1D case, a_0/L_0 = 1, t/τ_M = 0(0); = 1(1); = 2(2); = 3(3); = 8(4); = ∞(S).

(but not in steady-state) the photoinduced photorefractive lens is formed not in the center of the beam and the latter experiences some bending via this lens.

The maximal bending is observed at the time nearly equal to the Maxwell relaxation time and disappears in steady state. Depending on the sign of electric field and electro-optic coefficient this self-bending is accompanied by self-focusing or self-focusing.[1,2] Note that this effect can be remarkably stronger than the steady-state self-bending[3] as a result of diffusion recording mechanism. It is because for typical diameters of the beams used (tens of microns) effective diffusion field is dramatically inferior to the standard external electric fields applied to the sample (~0.1 and ~10 kV/cm, respectively).

Experiments were performed in cubic $Bi_{12}TiO_{20}$ (BTO) photorefractive crystals (grown at Hughes Research Center) where the drift length of photoexcited electrons can reach some microns in reasonable electric fields ~ 10 kV/cm. The focused beam of CW HeNe laser (λ = 633 nm, P = 7.8 μW, beam radius a_0 = 21 μm) was illuminating the sample and the time evolution of the output beam profile was detected by the photodetector (Fig. 1). To duplicate the efficient electric field in the sample volume (for a fixed, limited by the surface breakdowns applied voltage) the measurement procedure was performed in the following sequence. The negative (defocusing) voltage was applied first to the sample illuminated by the beam and after the electric field was compensated in the beam area the light was switched off and the voltage inversed. After this the light was switched on again and beginning from this moment we monitored the output beam. The typical beam profiles after the sample are given in Fig. 2, which demonstrates remarkable transient shift of the output beam center (and its self-focusing).

Our numerical simulation supports the model suggested above and proves to be in a reasonable agreement with the experimental results. In particular it allows one to estimate the average drift length of the photocarriers in BTO as L_0 ~ 3 μm (for effective electric field ~ 19 kV/cm). This means that remarkably bigger self-bending can be observed in BSO and GaAs samples with bigger $\mu\tau$ product. For example self-consistent solution for 1D (stripe-like) beam propagation in PRC taking into account finite drift of the carriers comparable with the beam semi-width (a_0/L_0 = 1) gives the following sequence of the output beam profiles (Fig. 3). As in the above experiment with BTO we observe here transient self-bending and self-focusing disappearing in the steady-state.

1. G. C. Duree *et al.*, Phys. Rev. Lett. **71**, 533 (1993).
2. M. D. Iturbe Castillo *et al.*, Appl. Phys. Lett. **64**, 408 (1994).
3. J. Feinberg, JOSA **72**, 46 (1982).

QThH4 **3:30 pm**

Higher-order space charge field effects on the evolution of spatial solitons in biased photorefractive crystals

S. R. Singh, M. I. Carvalho, D. N. Christodoulides, *Department of Electrical Engineering and Computer Science, Lehigh University, Bethlehem, Pennsylvania 18015*

Recently, photorefractive (PR) spatial optical solitons have been the focus of considerable attention.[1-6] Of particular interest are the so-called screening solitons that occur in steady state when an external bias voltage is appropriately applied to a PR crystal.[2,3] These soliton states are known to occur when the drift term dominates in the expression of the space charge field. In a recent study,[7] the effects arising from first-order diffusion terms have also been investigated. It was found that the PR soliton can experience adiabatically self-deflection that varies linearly with the applied electric field. However, recent experiments[8] suggest that this self-deflection can exceed that predicted by theory,[7] especially in the regime of quite high bias fields.

To account for this discrepancy, we in-

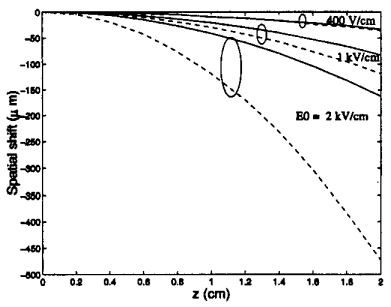

QThH4 Fig. 1 Comparison of spatial shift obtained by considering only the γ_1 term (solid curve) and (γ_1, γ_2) terms together (dashed curve) at different applied electric field strengths of E_0 = 400 V/cm, 1 kV/cm, and 2 kV/cm. A fundamental bright soliton with r = 10 is used at the input.

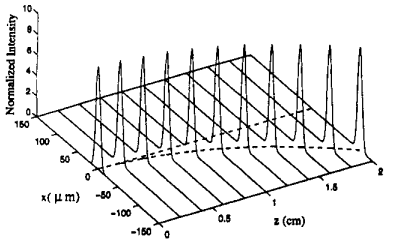

QThH4 Fig. 2 Evolution of $r = 10$ soliton at $E_0 = 1$ kV/cm under the influence of γ_1 and γ_2 terms.

vestigate the effects of other higher-order electric field terms on the evolution of bright steady-state solitons in PR media. To do so, let us consider the space charge electric field in the PR crystal, which is given by

$$E_{sc} \approx E_0 \frac{I_d}{I + I_d}\left(1 + \frac{\varepsilon_0 \varepsilon_r}{eN_A}\frac{\partial E_{sc}}{\partial x}\right) - \frac{K_B T}{e}\frac{(\partial I/\partial x)}{(I + I_d)} + \frac{K_B T}{e}\frac{\varepsilon_0 \varepsilon_r}{eN_A}\frac{\partial^2 E_{sc}}{\partial x^2}. \quad (1)$$

In Eq. (1), $I(x, z)$ is the power density of the optical wave front, I_d is the dark irradiance, e is the electron charge, and N_A is the acceptor density. Furthermore, E_0 is the electric field in the dark regions (at $x \to \pm\infty$) and $E_0 \approx V/W$, where V is the applied bias along the x coordinate and W is the x-width of the crystal. At moderately high applied bias V, the space-charge field is approximately given by[2,3]

$$E_{sc} \approx E_0 \frac{I_d}{I + I_d}. \quad (2)$$

To study the effects arising from higher-order terms such as $\partial E_{sc}/\partial x$ and $\partial^2 E_{sc}/\partial x^2$ in Eq. (1), we use the first-order solution of Eq. (1), *i.e.*, Eq. (2), and the other terms are obtained in an iterative fashion. As an example, let the photorefractive crystal be of the strontium barium niobate (SBN) type with its optical c axis aligned along x coordinate and n_e as its extraordinary index of refraction. It can be shown that in this case, the normalized envelope (U) of an optical beam linearly polarized parallel to the x-axis, $|U|^2 = I/I_d$, obeys the following paraxial evolution equation:

$$iU_\xi + \frac{U_{ss}}{2} - \beta\frac{U}{1 + |U|^2} + \gamma_1\frac{(|U|^2)_s U}{1 + |U|^2} + \gamma_2\frac{(|U|^2)_s U}{(1 + |U|^2)^3} - \gamma_3\frac{[(|U|^2)_s]^2 U}{(1 + |U|^2)^3} + \gamma_4\frac{(|U|^2)_{ss} U}{(1 + |U|^2)^2} = 0, \quad (3)$$

where the following transformations have been employed: $\xi = z/kx_0^2$ and $s = x/x_0$, where x_0 is an arbitrary scaling parameter. In Eq. (3), $\beta = (k_0 x_0)^2(n_e^4 r_{33}/2)E_0$ (r_{33} is the electro-optic coefficient involved, and $k_0 = 2\pi/\lambda_0$), $\gamma_1 = \beta\delta$, $\gamma_2 = \beta\varepsilon E_0^2$, $\gamma_3 = 2\beta\delta\varepsilon E_0^2$, $\gamma_4 = \beta\delta\varepsilon E_0^2$ where $\delta \equiv K_B T/ex_0 E_0$ and $\varepsilon \equiv \varepsilon_0\varepsilon_r/E_0 x_0 e N_A$. The fundamental bright soliton solutions of Eq. (3) can be obtained by setting all the γ perturbations to zero. In our previous study[7] the self-deflection effect was considered by including only the γ_1 term. With all terms present, we find that the γ_2 term in Eq. (3) further enhances the self-deflection process. This shift is found to increase considerably with the applied electric field strength. Figure 1 compares the self-deflection obtained by including diffusion (γ_1 term) alone and with γ_1 and γ_2 together. These results support the experimental observations of Ref. 8. Also shown in Fig. 2 is the evolution of $r = 10$ ($r \equiv |U|^2_{max}$) under the influence of higher-order terms at $E_0 = 1$ kV/cm. Moreover, for the range of applied electric fields below 2 kV/cm, the γ_3 and γ_4 terms were not found to have any significant impact. Similar results can also be obtained using perturbation analysis.

1. M. Segev, B. Crosignani, A. Yariv, B. Fischer, Phys. Rev. Lett. **68,** 923 (1992).
2. M. Segev, G. C. Valley, B. Crosignani, P. DiPorto, A. Yariv, Phys. Rev. Lett. **73,** 3211 (1994).
3. D. N. Christodoulides, M. I. Carvalho, J. Opt. Soc. Am. B **12,** 1628 (1995).
4. G. Duree, G. Salamo, M. Segev, A. Yariv, B. Crosignani, P. D. Porto, E. Sharp, Opt. Lett. **19,** 1195 (1994).
5. M. D. Castillo, P. A. Aguilar, J. J. Mondragon, S. Stepanov, V. Vysloukh, Appl. Phys. Lett. **64,** 408 (1994).
6. M. Shih, M. Segev, G. C. Valley, G. Salamo, B. Crosignani, P. DiPorto, Electron. Lett. **31,** 826 (1995).
7. M. I. Carvalho, S. R. Singh, D. N. Christodoulides, Opt. Comm. **120,** 311 (1995).
8. M. Feng Shih, P. Leach, M. Segev, M. H. Garret, G. Salamo, G. C. Valley, submitted for publication to Opt. Lett. (1995).

QThH5 **3:45 pm**

Modulation Z-scan technique in photorefractive crystals

P. A. Márquez Aguilar, J. J. Sánchez Mondragón, S. Stepanov, V. Vysloukh, *INAOE, Apartado Postal 51 y 216, Puebla, 72000, Mexico*

The Z-scan technique[1] proved to be a quite simple method (it uses one laser beam only) for characterization of different optically nonlinear media. Recently this technique was also successively applied to photorefractive crystals (PRCs) $Bi_{12}TiO_{20}$ (BTO) under an external DC electric field.[2] It was shown, however, that due to some point defects and inclusions that are typical for PRCs the standard Z-scan curves are characterized by a rather big spread of experimental points. Here we propose utilization of modulation version of this technique, which gives much better and more reproducible Z-scan curves in PRCs.

This approach is based on the ability to change the value, and in some cases

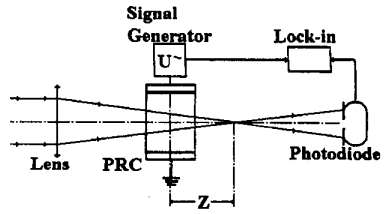

QThH5 Fig. 1 Schematic configuration of the modulation Z-scan characterization technique for photorefractive crystals.

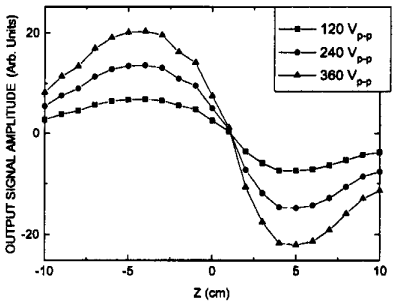

QThH5 Fig. 2 Typical modulation Z-scan curves obtained for three different amplitudes of sinusoidal modulation voltages in BTO at $\lambda = 633$ nm.

the sign, of the drift optical nonlinearity in PRC by changing some other parameters of the Z-scan experiment. In particular one can change the applied voltage sign, focused beam polarization, or intensity of the auxiliary uniform illumination of the sample.[2] In the first case the experimental setup is quite simple (see Fig. 1). Alternating electric field with an amplitude E_0 is applied to the sample, and it changes the sign of the drift nonlinearity periodically. The output signal in this Z-scan configuration is also detected at frequency of the field modulation Ω. This technique ensures easy utilization of temporal integration using a standard lock-in amplifier and reduces the influence of the point defects of PRCs (corresponding noise is transformed from the additive type in standard configuration into the multiplicative one).

Figures 2 and 3 represent experimental data obtained using a 2D focused beam of a cw HeNe laser for the BTO 9-mm-thick sample used earlier in Ref. 2 in standard (not modulation) Z-scan configuration. Figure 2 shows the typical Z-scan curves obtained for different amplitudes of the sinusoidal alternating voltage applied to the sample. One can see linear dependence of the curve amplitude versus the applied voltage value. Typical frequency dependencies of the output signal amplitude presented in Fig. 3 for different laser beam power demonstrate presence of some optimal modulation frequency. Indeed, the modulation frequency cannot be remarkably higher than the inverse Maxwell relaxa-